Turkish Journal of Earth Sciences (Turkish J. Earth Sci.), **Vol. 14**, 2005, pp. 123–143. *Copyright ©TÜBİTAK*

Stratigraphy of the Volcanic Products Around Nemrut Caldera: Implications for Reconstruction of the Caldera Formation

ÖZGÜR KARAOĞLU[1], YAVUZ ÖZDEMİR[2], A. ÜMİT TOLLUOĞLU[3], MUSTAFA KARABIYIKOĞLU[4], ONUR KÖSE[3] & JEAN-LUC FROGER[5]

[1] Dokuz Eylül University, Department of Geological Engineering, Bornova, TR–35100 İzmir, Turkey
(E-mail: ozgur.karaoglu@deu.edu.tr)
[2] Middle East Technical University, Department of Geological Engineering, TR–06531 Ankara, Turkey
[3] Yüzüncü Yıl University, Department of Geological Engineering, TR–65080 Van, Turkey
[4] Yüzüncü Yıl University, Department of Anthropology, TR–65080 Van, Turkey
[5] Blaise Pascal University, OPGC (Centre de Recherce Volcanologique), 5 Rue Kessler, 63038 Clermont-Ferrand, France

Abstract: The volcanological development of the Nemrut stratovolcano, located near the southwestern tip of Lake Van in eastern Turkey, is subdivided into three stages: pre-caldera, post-caldera and late stages. Two ignimbrite flows have been recognized in the pre-caldera stage. The earlier of the two occurred after basaltic lavas formed along extensional fissures. The latter, which forms the main subject of this paper, was a major flow associated with the development of the Nemrut caldera. The pyroclastic deposits of the Nemrut volcano in the pre-caldera stage are divided into three phases on the basis of palaeosols that separate them. The first phase includes plinian pumice falls and a pyroclastic flow deposit. The major ignimbrite occurs in the second pyroclastic phase and is here subdivided into three sub-layers based on colour, internal grading, size of pumice and lithic clasts, and the degree of welding. The third and last pyroclastic phase was dominated by plinian pumice and ash-fall deposits.

The occurrence of palaeosols between pyroclastic phases suggests that there were periods of inactivity between the eruptions. Formation of the Nemrut caldera is thought to have resulted from eruptions of pyroclastic materials with a volume of about 62.6 km^3.

Key Words: Nemrut, caldera, ignimbrite, pyroclastics, East Anatolia volcanism

Nemrut Kalderası Çevresindeki Volkanik Ürünlerin Stratigrafisi: Kaldera Oluşumu Açısından Anlamı

Özet: Van gölünün GB'sında (Doğu Anadolu) yer alan Nemrut stratovolkanı'nın volkanolojik gelişimi, kaldera öncesi evre, kaldera sonrası evre ve geç evre olmak üzere üç aşamada incelenmiştir. Nemrut volkanizmasına bağlı gelişen ve kaldera öncesi evreye ait iki ignimbirit birimi belirlenmiştir. İlk ignimbirit akması, açılma çatlakları boyunca gerçekleşen ve volkanizmanın ilk ürünleri olan bazaltik lav akmalarının ardından meydana gelmiştir. Nemrut kalderası'nın oluşumunu tetikleyen en önemli volkanik malzemelerden biri olan ana ignimbirit akması ise makalenin asıl konusunu teşkil etmektedir. Kaldera öncesi evredeki Nemrut stratovolkanına ait piroklastik ürünler, paleo-toprak gözlemleriyle 3 faz halinde incelenmiştir. İlk faz, pliniyen geri düşüşler ve pomza akışından oluşmaktadır. Ana ignimbirit ikinci faz içerisinde yer almakta olup pomza ve litik içerikleri, derecelenmeleri, büyüklükleri, kaynaşma dereceleri ile renkleri göz önünde bulundurularak 3 seviye halinde incelenmiştir. Üçüncü faz ise pliniyen pomza ve kül geri düşme ürünlerinden oluşmuştur.

Piroklastik ürünler içerisinde gözlenen iki ayrı paleo-toprak oluşumu, volkanizmanın kaldera oluşmadan önce belirli aralıklarda suskunluğuna işaret etmektedir. Nemrut kalderası oluşumunun 62.6 km^3 hacminde piroklastik malzemenin püskürmesi sonucu gerçekleştiği düşünülmektedir.

Anahtar Sözcükler: Nemrut, kaldera, ignimbirit, piroklastikler, Doğu Anadolu volkanizması

Introduction

The East Anatolia volcanism (EAV) began as a result of the collision of the Arabian and Eurasian plates and consequent compressional and extensional tectonic regimes (e.g., Yılmaz *et al.* 1998; Koçyiğit *et al.* 2001). Previous research has shown that the compressional tectonic regime created by the collision between the Arabian and Eurasian plates along the Bitlis suture zone has resulted in extensive crustal shortening (Şengör & Kidd 1979; Şengör & Yılmaz 1981; Dewey *et al.* 1986). Different types of volcanic eruptions have occurred including effusive to explosive-type volcanism, such as that represented by the Solhan volcanites, marking the initial effusive member, and the Nemrut volcanites, the final member, representing both effusive and explosive types which are considerated to be products of a so-called "neotectonic episode". The EAV is represented by shield volcanoes and stratovolcanoes which developed in an extensional tectonic regime. A compressional-extensional tectonic regime has triggered the formation of three stratovolcanoes (Nemrut, Süphan and Ağrı), a shield volcano (Tendürek), and the fissure-type volcanism of which there are many examples in eastern Anatolia.

A viable geological model for both the development of Lake Van and for the reconstruction of the neotectonic episode has long been sought (Şaroğlu & Güner 1981; Güner 1984). There is reportedly a strong relationship between the development of the Nemrut stratovolcano and the evolution of Lake Van (Karaoğlu *et al.* 2004).

The Nemrut stratovolcano hosts a well-developed caldera system and represents a typical example of volcanic activity initiated by N–S extension. Located to the north of Tatvan, this stratovolcano, which culminates at 2950 m, covers an area of approximately 36 km^2 (Figure 1), with its caldera situated near the southwestern tip of Lake Van (1648 m above sea level).

Previous Studies

A previous geological study of the Nemrut caldera by Özpeker (1973) suggested that volcanic activity began in the Quaternary. Five distinct phases were recognized which included (a) initial, (b) basic effusive, (c) acidic effusive, (d) caldera, (e) late-stage parasitic cone formation and within-caldera eruptions. The volcano-tectonics of the neotectonic episode and volcanogenic discrimination were investigated by Yılmaz *et al.* (1987). The older study clearly explained that the final oceanic lithosphere of the Tethyan realm was eliminated when the Arabian platform collided with Laurasia during the Middle Eocene, and that volcanic activity subsequently was initiated in eastern Anatolia (Şengör & Yılmaz 1981). The other detailed investigation on the volcanism of the east Anatolian plateau, mainly concerning the Quaternary volcanic cones of Ararat, Süphan, Nemrut and Tendürek, was carried out by Yılmaz *et al.* (1998). The authors noted that Ağrı is markedly subalkaline, Süphan mildly subalkaline, Nemrut mildly alkaline, and Tendürek strongly alkaline in character. They also explained the development of the Nemrut volcanic centre in terms of five distinct stages comprising (1) a pre-cone, (2) a cone-building, (3) a climactic, (4) a post-caldera and (5) a late stage.

The most crucial data for obtaining the thickness of Nemrut volcanics is drill-hole data. Three drill-holes (Nemrut 5, 7, 8) were operated for the geothermal fluid investigation project around Nemrut stratovolcano by TPAO-UNOCAL (1990a, b, c). Other critical data needed for deciphering the volcanic evolution of the east Anatolia volcanic province are reliable radiometric age determinations, currently lacking. Although still limited, some significant data have been become available since 1990. On the basis of trace-element data and isotope systematics, previous studies (Pearce *et al.* 1990; Notsu *et al.* 1995; Yılmaz *et al.* 1998; Keskin *et al.* 1998; Şen *et al.* 2004) suggested subduction-modified heterogeneous lithospheric mantle as the source of the eastern Anatolian volcanics, which have undergone varying degrees of crustal contamination on the way to surface. On the basis of major- and trace-element analyses, $^{87}Sr/^{86}Sr$ isotope analyses and K/Ar radiometric dating, Ercan *et al.* (1990) suggested that the time of initial collision was in the Middle Miocene. Notsu *et al.* (1995) suggested that volcanism in central and eastern Anatolia – active from Neogene to Quaternary time – was related to continental collision. In addition, Notsu *et al.* (1995) acquired radiometric age dates of 0.1 Ma to 0.01 Ma from volcanic-rock samples from the Nemrut stratovolcano. A study of the distribution of helium-isotope ratios in various tectonic provinces and historically active volcanoes of Turkey has revealed that mantle contribution reached a maximum level in the Nemrut stratovolcano of eastern Anatolia (Güleç *et al.* 2002).

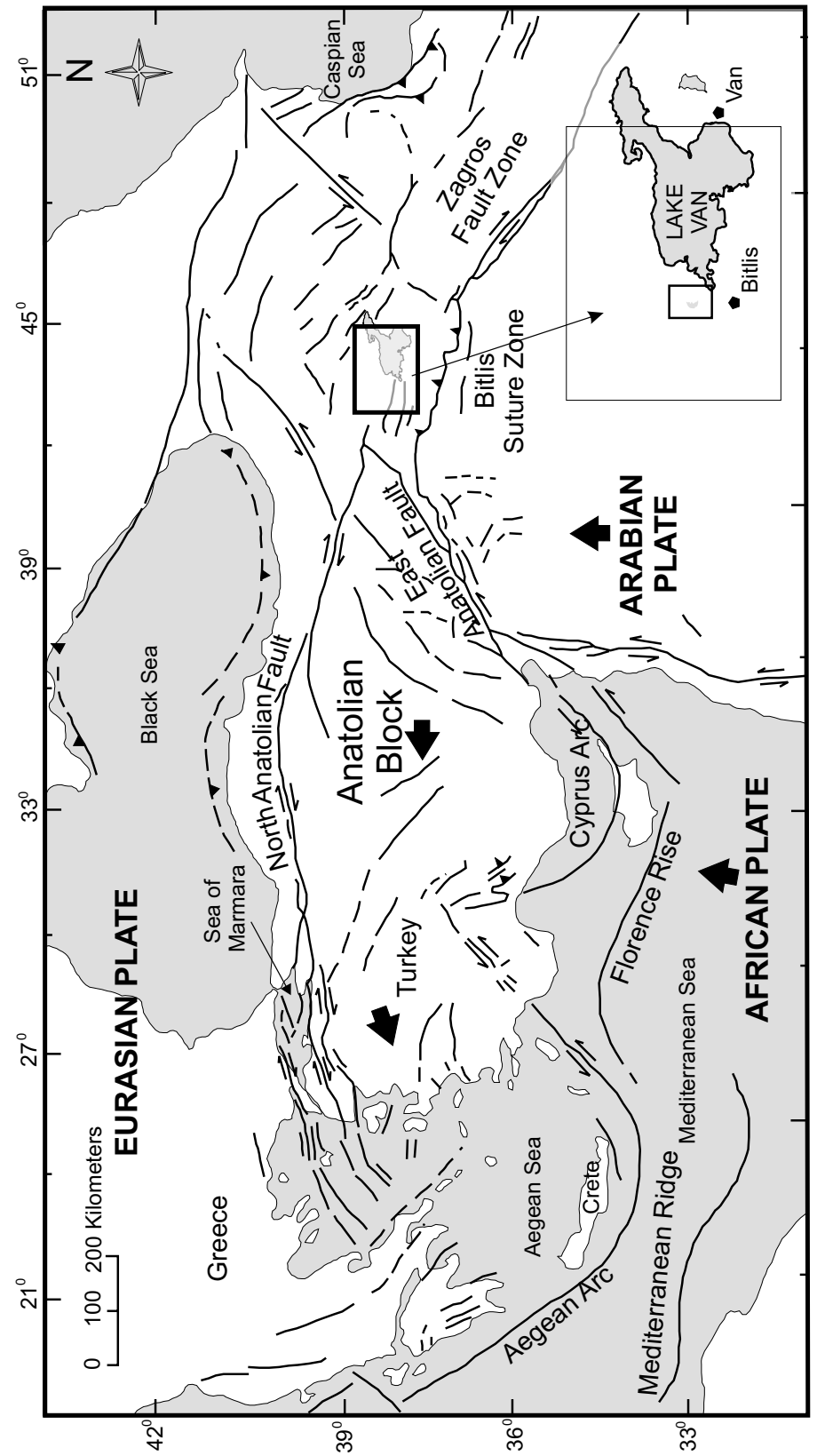

Figure 1. The study area and simplified tectonic map of Turkey showing major neotectonic structures and neotectonic provinces (from Bozkurt 2001, 2003).

Research of historical evidence from nearby volcanic systems was carried out by Karakhanian *et al.* (2002). Their research gave examples of Holocene-historical volcanism in the territory of Armenia and adjacent areas of eastern Anatolia and western Iran, discussing this volcanism in the light of remote-sensing data, field work, and historical and archaeological information. They concluded that these Holocene volcanic centres are situated within pull-apart basins controlled by active faults.

Mount Nemrut may be considered an active volcano on the basis of historical records. Aydar *et al.* (2003) investigated the evidence for future eruptions and possible impact areas of the Nemrut volcano on the basis of field observations. A digital elevation model and satellite images were also utilized. They calculated slope values at each point of the volcano flanks and the Heim parameters H/L, and found that the maximum depth of some valleys reach up to 200 m, and that the valleys were localized in three zones: the WSW flank where the deeper valleys are present; the SSE flank where the longest valleys are located; and the NNE flank where the valley depths and lengths are less important.

It becomes clear from the present literature that until recent times, most of the studies carried out in the area have basically been concerned with the general geological and geochemical characteristics of the Nemrut stratovolcano, and very little attention has been directed to the study of its volcanological evolution and pyroclastic materials. Therefore, there is considerable need to re-evaluate interpretations of both the mineralogic-petrographic, geochemical and physical volcanological data in the works pertaining to the evolution of the Nemrut stratovolcano.

The present study concentrates on facies analysis and comparison of cross-sections – with special attention to the pyroclastic deposits which triggered formation of the Nemrut caldera – and the goals of the present study include: (1) setting forth new insights concerning the physical evolution of the Nemrut stratovolcano, (2) ascertaining eruption type and the energy of the stratovolcano by evaluating the physical properties of the pyroclastic products, such as pumice and ash falls, (3) gathering volcanological clues that might elucidate the development of the Nemrut caldera through examination of the physical properties of the ignimbrites.

Volcanostratigraphy of the Nemrut Stratovolcano

Two recent detailed studies by Özdemir (2003) and Karaoğlu (2003) have provided further pertinent mineralogical-petrographical and geochemical data and produced four detailed geological maps at a scale of 1/25,000, pertaining to the volcanological evolution of the Nemrut stratovolcano (Figure 2). Based on the recent studies by Özdemir (2003) and Karaoğlu (2003), in this study we have identified three major evolutionary stages (pre-caldera, post-caldera and late stages) which have been further subdivided into several phases (Özdemir *et al.* 2005).

The Nemrut stratovolcano erupted various volcanic products (lavas, scoria and pyroclastics), covering the entire evolutionary range from basalt to rhyolite, during its long geologic history. These products developed under the influence of different dynamic forces and eruption types. In the following paragraphs, the physical evolution of the Nemrut stratovolcano is considered in terms of three stages, which are here defined as the pre-caldera, post-caldera and late stages.

The Pre-Caldera Stage

The pre-caldera stage consists of basaltic, trachybasaltic, trachyandesitic, trachytic lavas, trachytic ignimbrites (initial and main ignimbrite) and scoria observed at the south of the caldera. The exposures at the NW are located along NE–SW-trending left-lateral strike-slip faults.

Basaltic lavas filled up the Bitlis Valley completely and extended southward as far as to the town of Baykan, 80 km SW of the stratovolcano. The region was subjected to a N–S-directed compression, followed by N–S-directed extension during the Quaternary leading to the formation of extensional fissures and associated volcanism. The basaltic lavas, the first products of the Nemrut volcanism, indicate a low eruptive energy (effusion). The thickness of block lavas may reach up to 25–30 meters.

The trachytic ignimbrite is considered to have resulted from high-energy (explosive) eruptions. The trachytic lava extrusions at the northwest side of the caldera were of moderate energy and the basaltic lavas show blocky structure. The scoria layers that formed at the south of the caldera during cone building are generally associated with Stromboli-type eruptions. While basaltic-trachyandesitic lavas flowed from an extensional fissure to the south of the caldera, the trachytic-rhyolitic domes

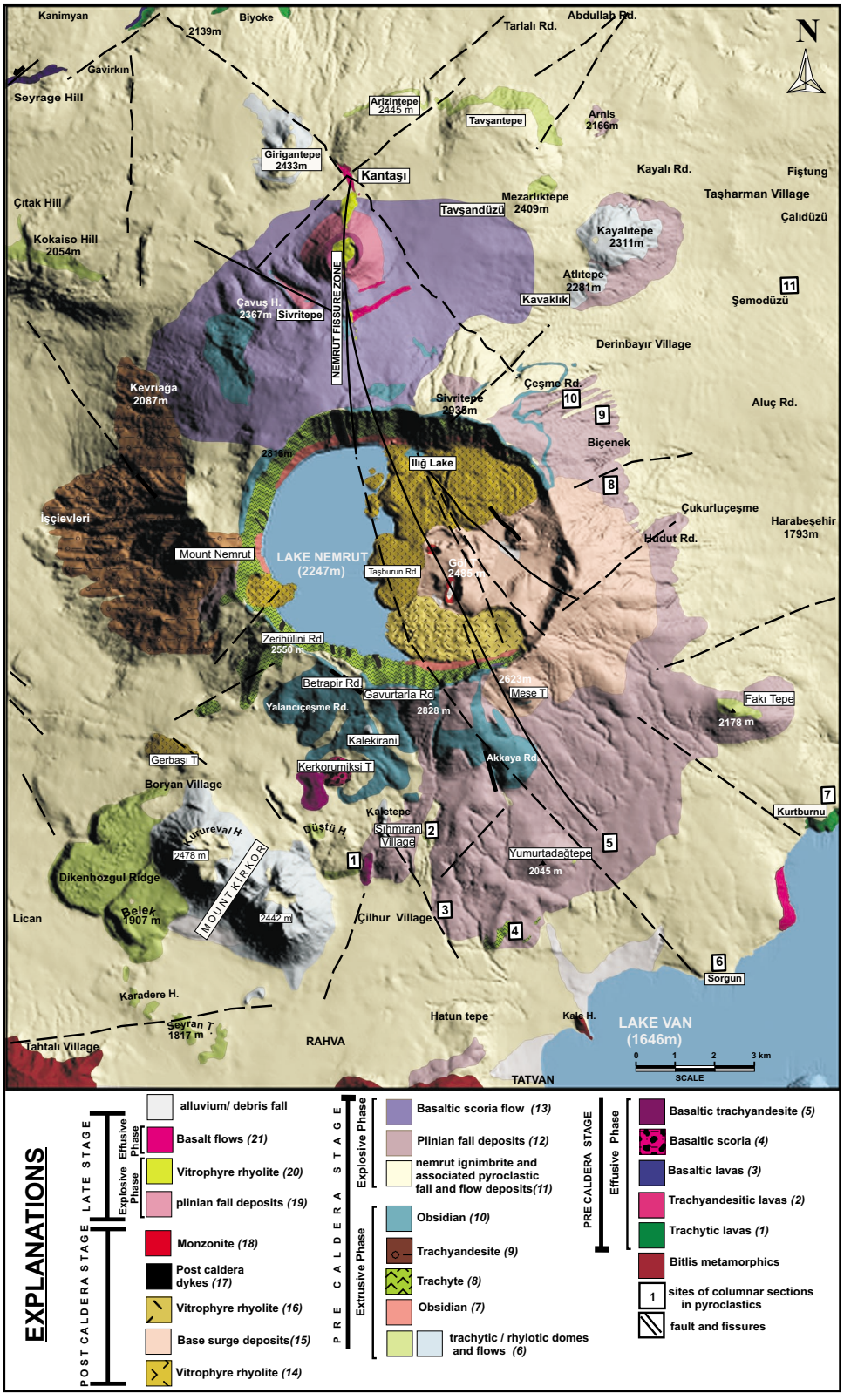

Figure 2. Geological and relief map of Nemrut stratovolcano.

that developed around the caldera in very large volumes represent examples of moderate-energy volcanism. The caldera rim is made up of trachytic-rhyolitic lavas, and around these lavas lie the main ignimbrite which indicate high-energy eruptions following cone building. Cone building was completed mainly by basaltic scoria flows on the northern side of the caldera. Considering the characteristic features of the distribution of the scoria flows in the area, their structural-textural relationships, and their mineralogical composition, these flows are considered to have resulted from moderate-energy eruptions.

The Post-Caldera Stage

Following the ignimbrite, a new process – defined here as a post-caldera stage – began. The post-caldera stage consists of four different phases: early vitrophyric rhyolite flows, phreatomagmatic base-surge eruptions, late vitrophyric rhyolite flows, and post-caldera dykes (Özdemir *et al.* 2005). The base-surge deposits of this stage are exposed in the eastern part of the caldera over an area of 13 km^2 and largely cover exposures of the early vitrophyric rhyolite flows (Figure 2). The base-surge deposits consist chiefly of ash, with only minor amounts of lapilli-sized lithic and pumice fragments. The lithic fragments and pumice clasts reach 6 cm in size. The deposits expose dune bedding and bomb-sag features, 40 cm in size (Özdemir *et al.* 2005).

Post-caldera dykes are located at the western, southern and northern walls of the caldera (Özdemir *et al.* 2005). The ones at the western and southern walls are felsic, whereas the one at the northern wall is basic in character. The felsic dykes are 1.5–10 m wide and 10–30 m in length, and cut the obsidian and trachytic flows of the caldera wall. The strike varies between N80°W and N60°E (Özdemir *et al.* 2005). A basic dyke, 50 m wide and 300 m in length, cuts all the units along the caldera wall. It has N–S strike which is related to the N–S-trending extensional fault system (Figure 2). The field observations indicate that a vertically propagating dyke may become arrested at a weak contact (cf. Gudmundsson 2002).

The Late-Stage

The late-stage is characterized by both explosive and effusive products. They are exposed along a 5-km-wide zone north of the caldera, located at a distance of 1.5 km from the caldera wall (Özdemir *et al.* 2005). The late-stage activity occurred through the N–S-trending Nemrut fissure zone, the width of which is up to 4 m at the Kantaşı locality (Figure 2).

Pumice fall deposits in the vicinity of Sivritepe comprise the first products of the explosive phase and are overlain by vitrophyric rhyolite flows exposed in topographic lows which are aligned along a 5-km-wide zone. The topographic lows are ellipsoidal in shape, with long and short axes having lengths of 100–725 m and 25–625 m, respectively. Volcanic bombs, 20 cm to 1 m in diameter, are typical features of the lava flows (Özdemir *et al.* 2005).

The last known lava flows in Turkey occurred around the parasitic cone and along the extensional fissure in the northern part of the caldera (Figure 2). According to Oswald (1912), eruption of the lavas occurred in 1441 A.D.; however, Aydar *et al.* (2003) – based on an Arabic book (Serefhan 1597) that gives an eyewitness description of the last eruption of the Nemrut volcano – suspect even younger eruptions.

Ignimbrites from the Nemrut Stratovolcano

We have studied the ignimbrites related to the Nemrut caldera at 65 locations in the field area – which takes in some 2500 km^2 – measuring the size of clasts and pumice elongation ratios, and studying characteristic type sections from the ignimbrites.

Two distinct types of ignimbrites have been observed from the Nemrut stratovolcano: the initial and the main ignimbrites. The initial ignimbrites were found in Bitlis Valley, situated to the south of the volcano, as well as to the northeast of the caldera. The main ignimbrite deposits are characterized by multiple eruption stages and comprise acidic volcanic materials belonging to a pre-caldera stage (Figure 2). The pyroclastic deposits of the Nemrut volcano in the pre-caldera stage are divided into three stages on the basis of palaeosols observed within the pyroclastic deposits. Each unit is identified by colour, internal grading, size of pumice fragments, lithic clasts, and degree of welding. The term '*Nemrut Ignimbrite*' (NI) was recently used for the so-called "welded" unit within the main ignimbrites (Özdemir 2003).

Initial Ignimbrite Eruption

The initial ignimbrite, whose thickness exceeds 40 m locally, overlies early basaltic lava flows. The maximum

thickness is ~42 m observed in the vicinity of Baykan (outside the study area, shown in Figure 2). The deposits extend 10 km to the southwest from the city of Bitlis. Bitlis itself is situated on the columnar-jointed ignimbrite. The initial ignimbrite is characterized by physical variations related to moderate degrees of welding. Pumice flow deposits (comprising more than 50% of pumice clasts) have been observed beneath the ignimbrite (Figure 3). Pyroclastic flow deposits occur in the Bitlis Valley, but are best studied as far as 13 km northwest of the caldera. In the flow unit, the maximum pumice fragment size is 15 cm.

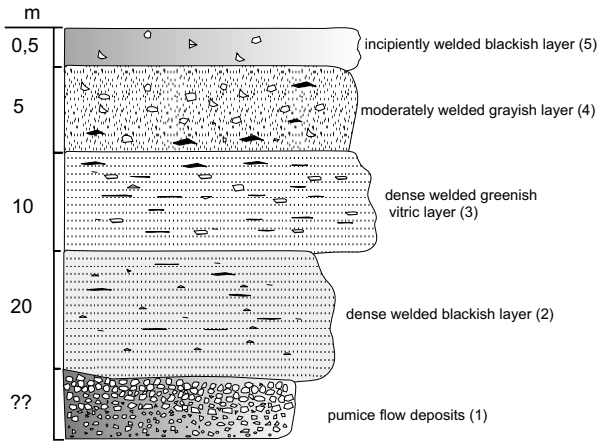

Figure 3. Type section of the 'initial ignimbrite' in the Bitlis Valley (not to scale).

The basal ignimbrite is black and welded. The size of lithic clasts reaches a maximum of 1 cm, and lithic and pumice fragments exhibit complex textures. The ignimbrite has glassy texture and contains fiammes, with the flattening ratio of the five largest pumice fragments is 0.2/3. A 20-m-thick black, glassy horizon is observed only in Bitlis Valley.

The subsequent ignimbrite (green layer) is distinctive with its glassy-welded texture and its columnar jointing, similar to the black horizon below. This layer encloses many fiammes, and its colour varies from green to greenish-grey from bottom to top. The flattening ratio of the five largest pumice fragments is 2/25. This layer is 10-m thick, and the maximum lithic clast size is 1.5 cm. The green ignimbrite layer is also observed 11 km north of the caldera at the Güzelsu location, west of the caldera at the Aşağı Kolbaşı location, and in the Bitlis Valley.

The third ignimbrite layer, about 5-m thick with a maximum pumice-fragment size of 3 cm, is characterized by an upward decrease in the degree of welding and flattening ratios. The size of the lithic clasts ranges up to 2 cm.

The uppermost unit is a non-welded, blackish ignimbrite layer, and is observed at the top of the sequence. Herein, a texture characterized by pumice and lithic fragments is more obvious than in lower parts of the sequence. A rock density of 2.495 gr/cm^3 has been obtained from this unit.

The Main Ignimbrite

The main ignimbrite body is clearly separated from the underlying deposits by a palaeosol that is exposed in several places. Based on palaeosols within the pyroclastic materials, plinian eruptions occurred in three phases (Figures 4 & 5).

Phase 1. This phase was deposited before the Nemrut Ignimbrite, and comprises pyroclastic fall deposits and pumice flow deposits (Figure 5). The latter are restricted to isolated outcrops in the study area. Pyroclastic fall deposits, which preceded the ignimbrite, have been divided into two units (U1, U2) (Karaoğlu 2003) separated by ash-fall deposits, 8.5-m thick. Scoria fragments (S), ash-fall deposits (A) and pumice-fall deposits related to the Nemrut Ignimbrite (P.F.D) occur northwest of the caldera. These pyroclastic materials only occur in restricted parts of the study area; we observed them mainly in deeper valleys.

Unit 1 (U1), the initial deposit, comprises a 3-m-thick, white, pumice fall (P1), with a maximum clast size of 4 cm. P2 has an average thickness of 1 m, exhibits strong indurations, and contains some lithic fragments having a maximum size of 6–7 cm. This unit also contains radially portioned pumice fragments. Both P1 and P2 are exposed outward from the source to about 5.5 km away. Stratigraphically higher P3 is black, coarse grained, fragmental, and quite rich in lithic fragments, with a maximum clast size of 7 cm. Approximately 80-cm thick, P3 is similar to P2 and also contains radially partitioned pumice fragments. This horizon is best exposed near Çilhur and Şıhmiran villages. Pumice flow deposits have been observed only along deep valleys atop plinian fall deposits (P1, P2, P3) SSE of the caldera. Furthermore, it

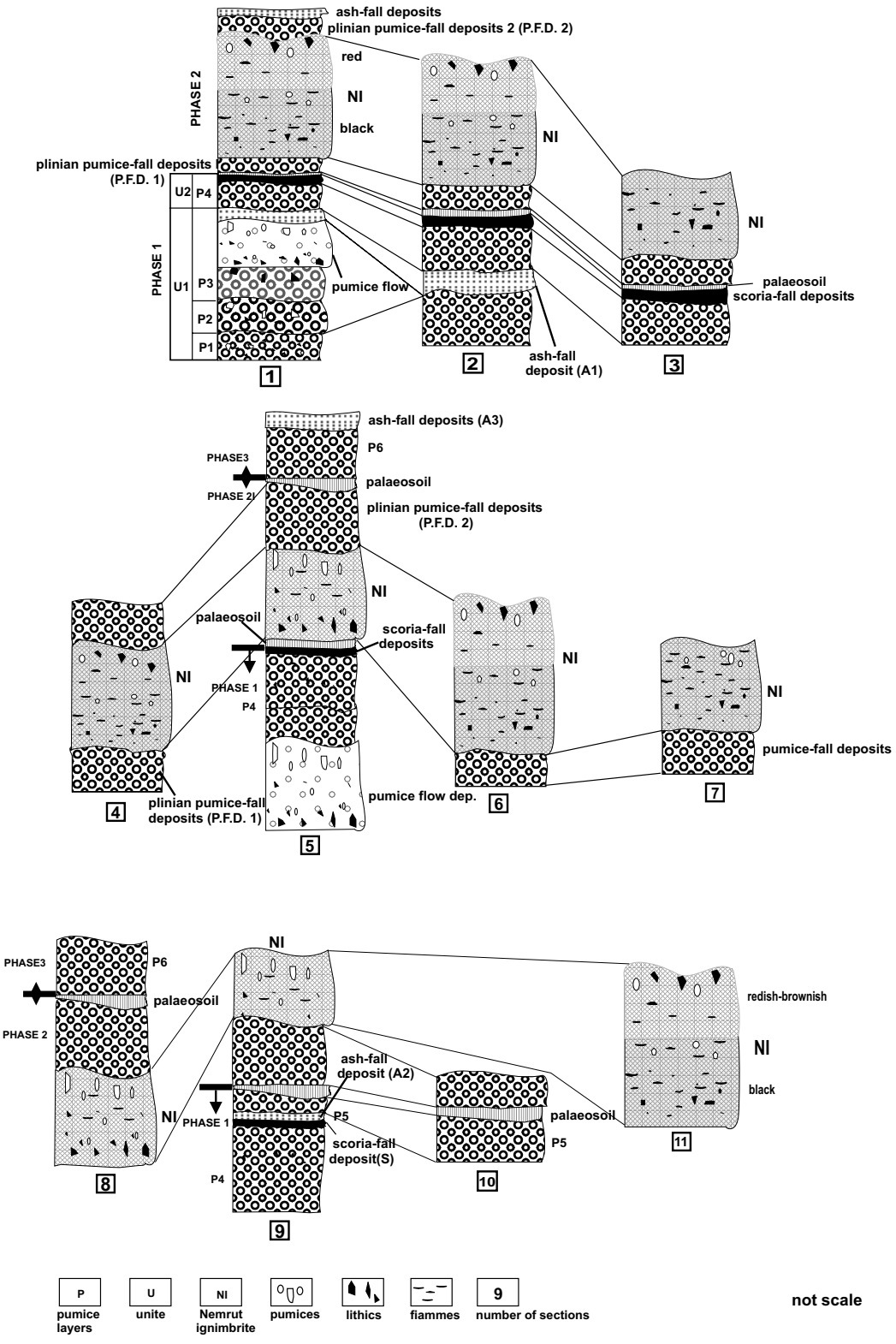

Figure 4. Depositional sequence of the 'main ignimbrite' (Nemrut stratovolcano pyroclastics; not to scale).

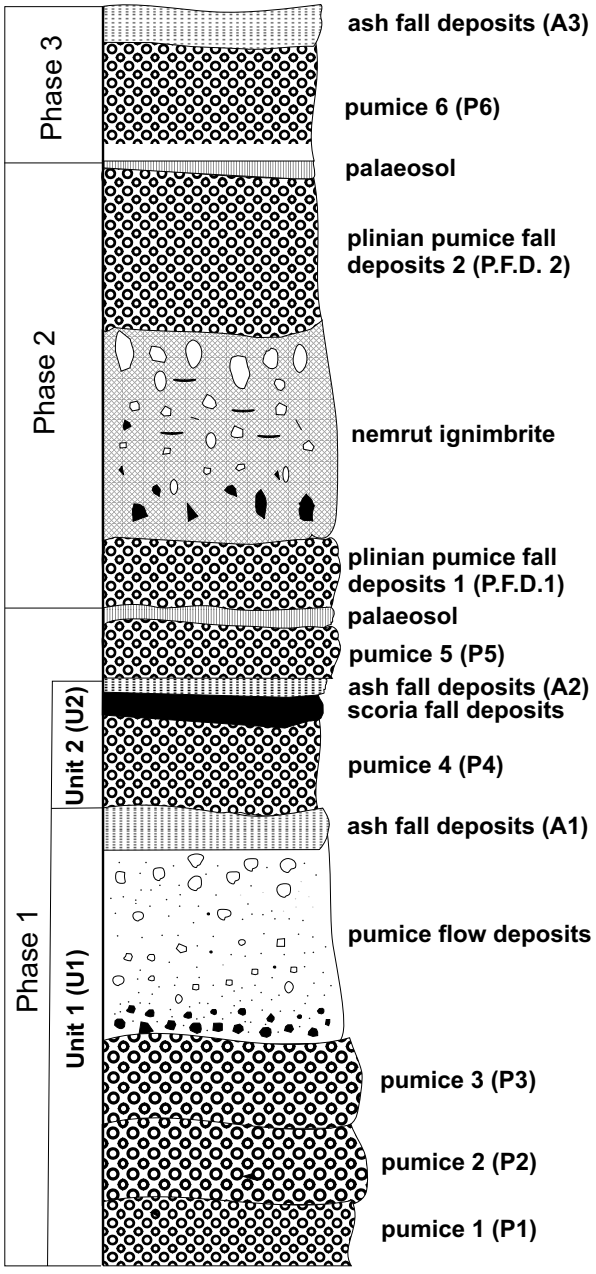

Figure 5. The generalized stratigraphic section of the Nemrut stratovolcano tephra sequence showing three phases during the main ignimbrite (not to scale).

was deposited at cross-section number 5, south of the caldera, and a few individual exposures occur on the ridges S of Şıhmıran village and NE of Yumurta Tepe. Subsequently, this deposit was covered completely by the Nemrut Ignimbrite.

The pumiceous pyroclastic flow deposit – with an overall reverse grading of pumice, and normal grading of lithic fragments – is described as a standard ignimbrite flow unit by Sparks (1976). Locally, gas escape pipes are observed in the uppermost parts of the deposit. Lithic components, with a maximum particle size of 5 cm, comprise trachyte, basalt and rhyolitic co-magmatic obsidian fragments. The uppermost part of the deposit is marked by an ash layer (A1), 20-cm thick. Internal cross-stratification and dune bedding indicate deposition from laterally fast-moving clouds.

Unit 2 (U2) begins with a pumice-fall deposit (P4). The maximum clast size of the radially partitioned internal pumice is 7 cm, and the gas cavities are oval to spherical. This unit also contains some lithic fragments, with maximum clast sizes of 0.3 cm. U2 is white to light green, and has a finer average particle size than U1. Additionally, scoria fall deposits immediately overlie U2.

In the study area, the scoria fall deposits are black and have a maximum clast size of 1 cm. The thickness of the exposed scoria varies considerably; for example, north of the caldera and at source, the scoria is 3-m thick, while it is only 20-cm thick 17 km south of the caldera. In the northern area, the maximum clast size within the scoria fall deposits is 1 cm, with lithic fragments averaging 5 mm. Furthermore, these deposits are supported by a black-brown ash matrix.

The subsequent deposit, 10-cm thick, overlies the scoria fall deposits. It consists of very dark, fine-grained ash particles, together with lithic fragments up to 2 cm in size – the most notable aspects of these deposits. The ash-fall deposit (A2) is well-sorted. A2 is overlain by a 15-cm-thick, white pumice unit (P5). Locally, there are marked transitional contacts between P5 and A2 (Figure 6).

Phase 2. This phase comprises Nemrut Ignimbrite and related plinian fall deposits: P.F.D. 1 and P.F.D. 2. The ignimbrite covers a mapped area of more than 616 km^2. At its base, a 25–30-cm-thick palaeosol occurs, separating phases 1 and 2 (Figures 5 & 7a). Observed in various places both north and south of the caldera, this palaeosol clearly separates phases 1 and 2, and is interpreted to reflect a hiatus in volcanic activity. Although these deposits were deposited just before the NI, they are only observed to the NE and SE of the

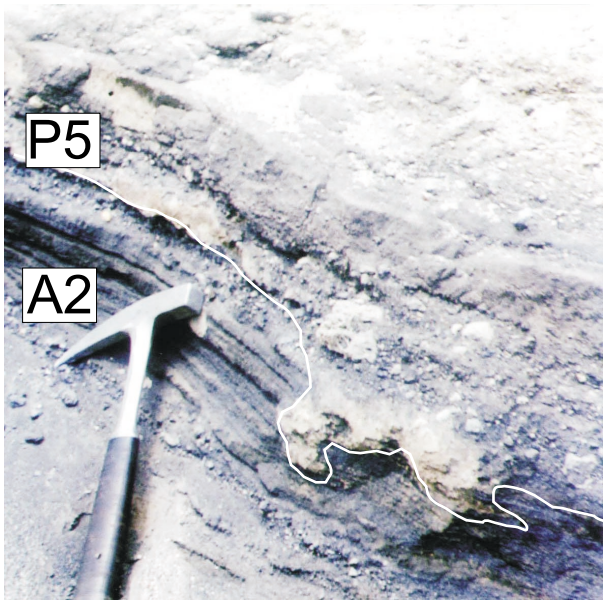

Figure 6. Penetration of pumice-fall deposits into underlying ash. Key to abbreviations: P5– pumice layer-5; A2– ash layer-2.

caldera. To the SE, they are clearly identified at about 1.5 km SW of Fakı Tepe Dome in a pumice quarry. An approximately 1.5-m-thick white pumice-bearing unit (P5) contains pumice fragments up to 2 cm in maximum dimension, and is overlain by locally altered, grey-brown plinian fall deposits (P.F.D.1) roughly 80-cm thick. P.F.D. 1 contains pumice fragments up to 4 cm in size; the white-to-grey pumice fragments are characterized by spherical gas cavities. The P.F.D.1 and NI are separated by a sharp contact (Figure 7b).

Northeast of the caldera, at the Çukurluçeşme location and in a nearby valley, the maximum dimensions of pumice fragments are as large as 5 cm, but up to 8 cm in the valley as it is traced to the south. At this location, the pyroclastic materials are observed as conformable to the slope of the palaeotopography, and P.F.D.1 is ~1.5-m thick. Moreover, layering is best exposed at this location (Figure 7c). Within P.F.D.1, buff-brown and black layers consisting of ash that separate pumice and lithic clasts are observed, indicating short-lived laterally moving clouds released from the centre. Layers within the pumice deposits are of various thickness, and the clast sizes of the pumice and lithic fragments (the latter derived from the caldera rim) vary from mm- to cm-scale. Laminae composed of black ash and lithic fragments vary at a millimetric scale. Towards the north from this location, evidence for pyroclastic surge deposits is present. Black pumice deposits occur over a 15–20 km^2 area on the eastern slopes of the caldera along the Ahlat road, overlying a different type of pumice-fall deposit (P.F.D.2). The black pumice fragments occur along sharp contacts and are thought to have been related to the pre-caldera scoria flow deposits at the uppermost part of the northern caldera wall.

Throughout the study area, the Nemrut Ignimbrite is recognized and is subdivided into three layers: bottom, middle and top (Figure 8). The ignimbrite represents the welded part of the pyroclastic flow deposits. The Nemrut Ignimbrite overlies the metamorphic basement 9.5 km south of the caldera, and low-lying areas and valleys are filled with NI. While clast sizes of pumice and lithic fragments in the vicinity of the caldera are rather large, they become smaller away from the caldera. This ignimbrite covered a large part of the study area, overlying pre-caldera lava flows, including dome structures.

The phenocryst assemblage of Nemrut Ignimbrite is made up of sanidine, plagioclase, clinopyroxene and hornblende. The deposit as a whole shows porphyritic texture and exhibits a moderate to high degree of welding. A prominent feature of the deposit is its vertical and lateral colour variations, with black, grey, brown and reddish-brown hues. Generally speaking, black and brown materials typify bottom layers, whereas red and grey materials are characteristic of top layers. In places, these various-coloured materials have transitional contacts.

The bottom layer is 1–7 m in thickness and black, enclosing only rather small clasts, and exhibits laterally varying degrees of welding from the north to south end of the caldera. A density of 2.625 gr/cm^3 was obtained for the bottom layer. This unit is termed 2a (cf. Cas & Wright 1988). To the north, between Kayalı Hill and Atlı Hill, the bottom layer is notable as the most densely welded in the region. This ignimbrite is up to 4–5 m in thickness, and has been observed in a valley having a 45–50° slope angle and length of 150 m where it is in contact with a trachytic dome. It is notable that extremely dense welded ignimbrite of the bottom layer is identified only 5 km northeast of the caldera. For example, dense welded ignimbrite is present NE of the caldera at the peak of Tavşan Tepe where it is exposed over a 1.5–2 km^2

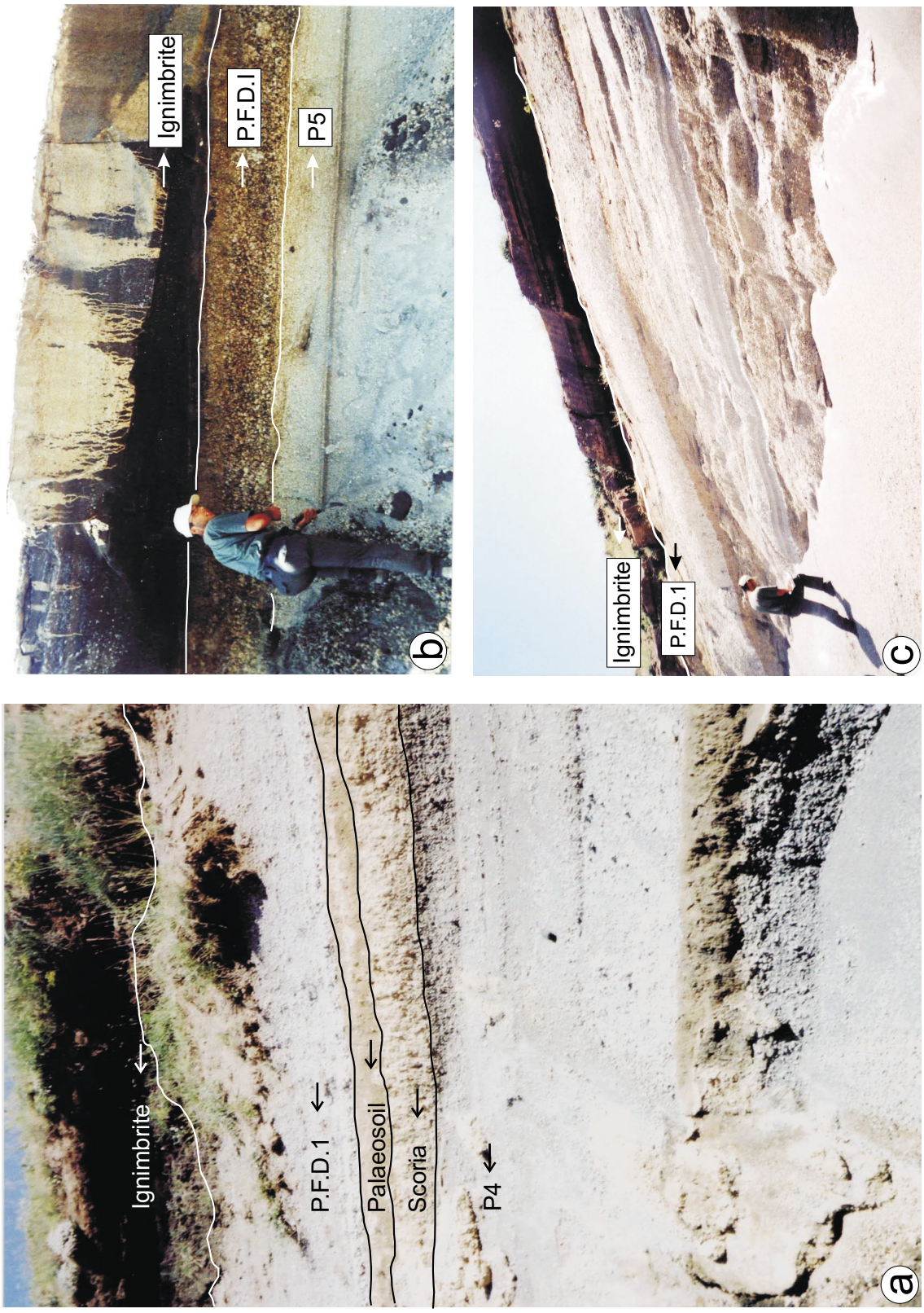

Figure 7. Photographs of Nemrut stratovolcano pyroclastics. **(a)** Phase 1 and Phase 2 pyroclastics, 6 km away from south of the caldera (hammer for scale); **(b)** Phase 2, plinian-fall deposits and ignimbrite at south of the caldera (Sorgun Village, person for scale); **(c)** Phase 2, plinian-fall deposits and ignimbrite north of the caldera. Key to abbreviations: P.F.D.1– plinian pumice-fall deposits 1; P4-5– pumice layer-4-5; NI– Nemrut Ignimbrite.

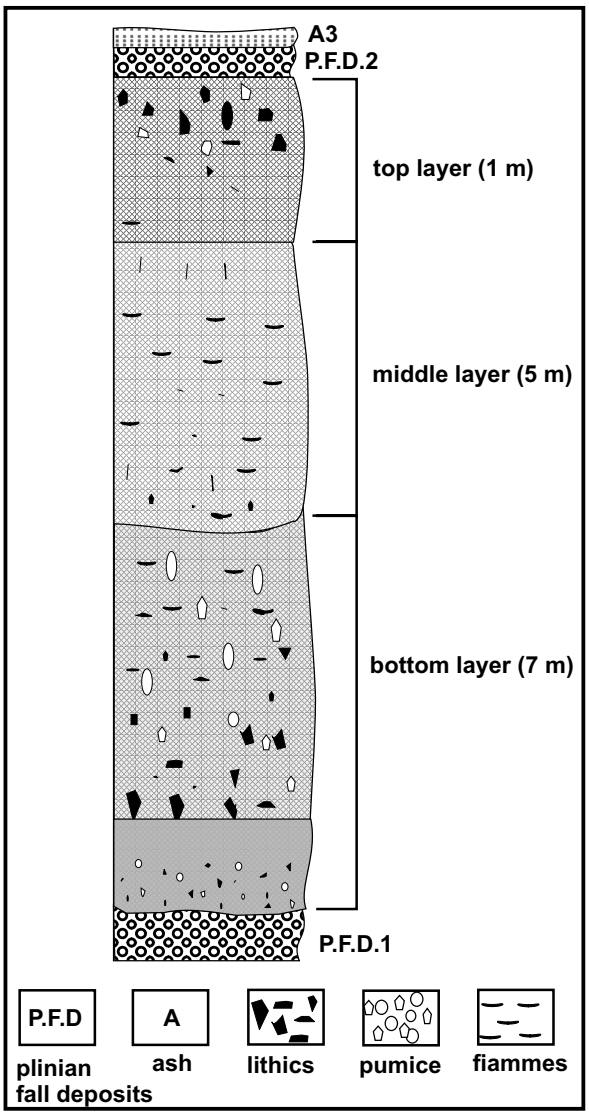

Figure 8. Type section of the Nemrut Ignimbrite (not to scale). Key to abbreviations: P.F.D.1-2– plinian pumice-fall deposits 1-2; P5– ash layer-3.

area. This flow is 2–3-m thick, situated between a trachytic dome and the top layer of the Nemrut Ignimbrite. At the Kavaklık location NNW of the caldera, dense welded ignimbrite is clearly observed in 3- to 4-m-deep stream valleys. Moderately welded material belonging to the bottom layer is exposed to the south of the caldera. This unit comprises scoria, pumice, trachyte and rhyolitic obsidian clasts. The maximum particle size for pumice clasts varies between 2 and 3 cm, whereas that of lithic clasts reaches 4 cm. Although it was not possible to observe this unit throughout the study area, it is widespread and easily identified at two locations south of the caldera, namely ESE of Şıhmıran Village and SE of Yumurta Dağ – the latter being the location of its maximum thickness, 7 m.

The middle layer of the Nemrut Ignimbrite comprises grey, brown, and red, moderately welded material. A density of 2.633 gr/cm^3 was obtained for the middle layer. Defined as a lahar by Güner (1984), this stage has an average thickness of about 7 m in all and is clearly identified south of the Kirkor Dome at Tahtalı village and north of Hatun Tepe. Matrix-supported, poorly sorted pumice clasts occur within this unit (Figure 9a). The upper parts of this layer are densely welded and contain trachytic and rhyolitic-obsidian lithic clasts. The maximum size of the pumice clasts is approximately 30 cm, and rounded lithic fragments are up to 20–25 cm. Red and reddish parts are characterized by a high degree of welding with some fiammes. The average thickness of the reddish interval is 5 m, and the fragment sizes of the lithic and pumice clasts are small relative to those of the lower parts of the middle layer.

North of the caldera, the middle layer displays quite different characteristics; for example, the material exposed between the Derinbayır and Şemodüzü locations is, in many places, red and brown, and its thickness reaches 5 m in deeper valleys. The welded interval of the NI that overlies the middle layer is 1–2-m thick, and contains 4–5-cm pumice clasts and minor amounts of 1–50-cm lithic fragments. There is marked alteration in some parts of this interval. Within these lithic-clast-rich intervals, lithic clasts are at mm–cm scale, whereas pumice clasts are at cm–dm scale. The latter are black due to recrystallization. Generally speaking, widespread ignimbrites belong to the middle layer. Pumice fragments are recrystallized due to welding and have been flattened by compaction; consequently, this unit contains well-developed fiamme structures (Figure 9b). In black layers, recrystallized pumice fragments are abundant. In the transition from the lower to middle parts of this unit, the particle size of the lithic and pumice clasts decreases.

The top layer is exposed only within a limited area; for example, SW of the caldera at Boryan Village, north of the Kirkor Dome, and on the southern slopes of the caldera itself. Approximately 1 m thick, this stage exhibits a low degree of welding. A density of 2.662 gr/cm^3 was obtained for the top layer. The upper parts of this stage are grey to greyish brown and contain rounded and altered scoria and pumice clasts, with average particle

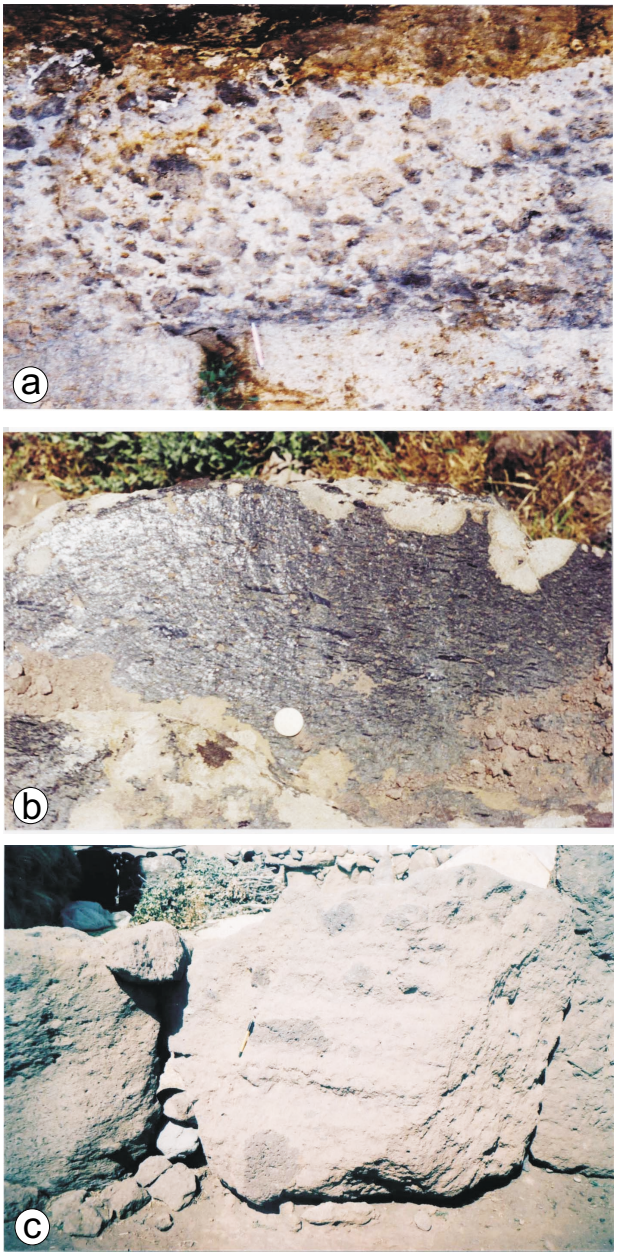

Figure 9. Photographs of the Nemrut Ignimbrite. **(a)** Middle layer, composed of pumice poorly sorted with supported matrix (pen for scale); **(b)** middle layer, fiammes within the middle stage of the ignimbrite (coin for scale); **(c)** top layer, recrystallized pumices (pen for scale).

sizes of 10–15 cm. Moreover, the inner parts of this stage are altered and rich in brownish and greyish lithic material. Due to a low degree of welding, the clasts are dispersed with ash matrix. In some places, the unit contains recrystallized pumice fragments. The sizes of scoria and pumice clasts increase with proximity to the caldera, and the upper part of this stage is characterized by poor grading (Figure 9c). Lithic clasts exhibit clast-size variation at different localities: 2–3 cm northwest of the caldera (Çukurluçeşme); 1–1.5 cm 8 km north of the caldera (Taşharman village); and 1–1.5 cm 5 km north of the caldera. Within this ignimbrite unit, caldera-wall clasts, especially rhyolitic and trachytic fragments incorporated during eruption, are also present. Generally, trachytic fragments are larger nearer the caldera wall. Ignimbrites situated on the NNW caldera wall (at Sivri Tepe and on Çeşme Ridge) contain country-rock clasts that are up to 5–6 cm in size, and to the NE at Derinbayır Village, clasts are 3–4 cm in size.

Following eruption of the Nemrut Ignimbrite, all dome surfaces were covered by ignimbrite, but this unstable material was subsequently eroded. The Nemrut Ignimbrite initially overtopped the Kirkor, Arizin and Tavşan domes, but was eroded from dome slopes having 55–60° slope angles (Figure 10). E–W- and NE–SW-oriented river systems developed in ignimbrites that filled low areas NW of the caldera. Within these stream valleys, the NI is locally 5–6-m thick, and the size of lithic clasts therein is on the order of 1.5 cm.

Subsequently, the Nemrut Ignimbrite was covered by P.F.D.2: the thickness of P.F.D.2 varies from 30 cm to 2.5 m (Figures 5 & 11a). The pumice-fall and pyroclastic surge deposits cover an area of at least 60 km^2. This unit is generally normally graded, but contains lithic fragments that reach a maximum size of 3 cm. Pumice fragments therein are grey to white, with maximum clast sizes reaching 9 cm. The P.F.D.2 is overlain by ash-fall deposits, as observed south of the caldera, and the ash-fall deposits reach a thickness of 10 cm. Northeast of the caldera, size variation of pumice and lithic fragments was observed in plinian fall deposits which both pre-date and post-date the NI.

Phase 3. A 3–5-cm-thick reddish-brown palaeosol, situated between Phases 2 and 3, has been observed in deep valleys south of the caldera (e.g., near Şıhmiran Village). The palaeosol indicates a dormant period following the main ignimbrite stage.

Pumice (P6) in this phase is grey and white and has a maximum fragment size of 3 cm (Figures 5 & 11b). This pumice unit is characterized by spherical gas cavities. P6

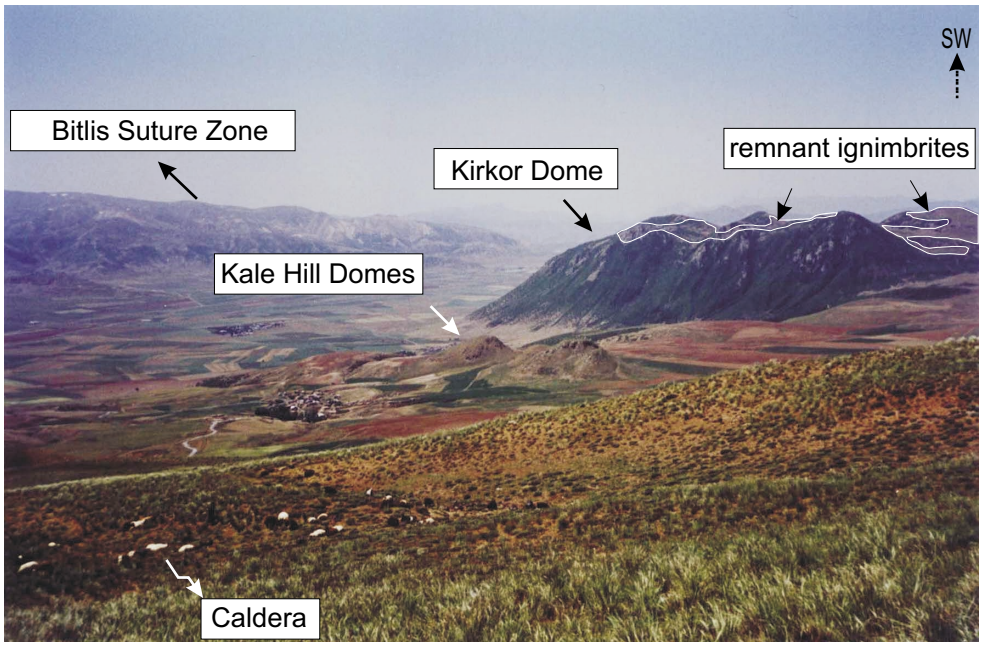

Figure 10. Remnant ignimbritic deposits on the Kirkor Dome.

Figure 11. (a) Nemrut Ignimbrite and plinian-fall deposits in the northeastern part of the caldera; (b) P.F.D.2 and Nemrut Ignimbrite from the southeastern part of the caldera. Key to abbreviations: P.F.D.1-2– plinian pumice-fall deposits 1-2 (person for scale).

is overlain by A3, and has an aerial extent of about 30 km^2.

Drilling Data

Three drill holes (Nemrut 5, 7, 8) were operated for a geothermal-fluid investigation project around Nemrut stratovolcano by the TPAO and UNOCAL companies (Figure 12). Here we will focus on the thickness of the pyroclastic units, based on the drill-hole data. According to this drilling project data: (1) the Nemrut 7 drill hole (elevation: 1299 m) was located 13 km west of the caldera rim; the tuff unit cut was around 98-m thick, after which was cut a trachytic layer having a thickness of

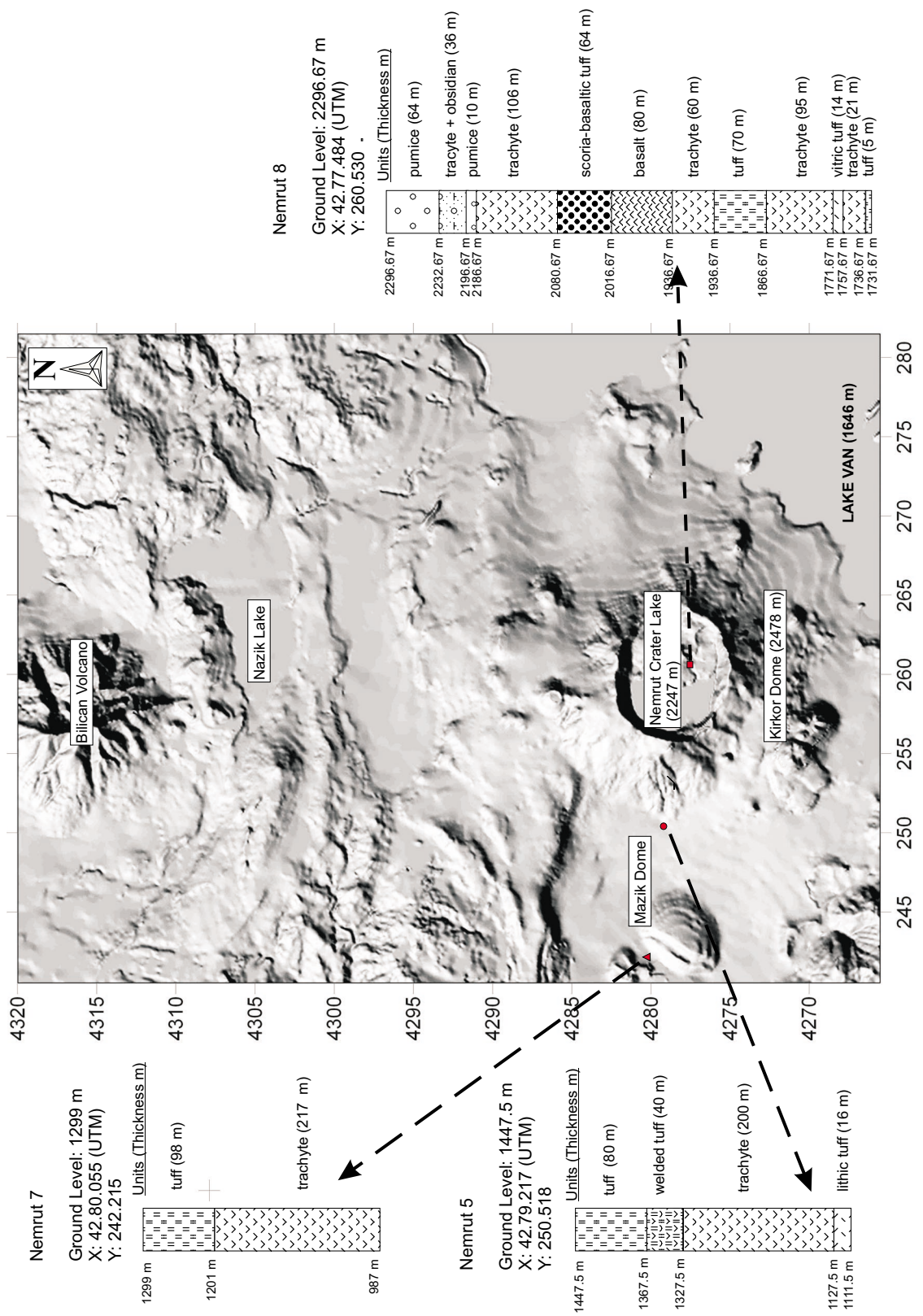

Figure 12. Shaded relief map and showing drill holes around Nemrut stratovolcano (scale: 1/100,000).

217 m (TPAO & UNOCAL 1990a; e.g., Ömer Şahintürk, pers. comm. 2005), (2) the Nemrut 5 drill hole (elevation: 1477.5 m) was located 6 km west of the caldera rim; the thickness of the tuff unit is around 80-m and includes some obsidian fragments. After this unit, a welded tuff layer of 40 m thickness was cut. Underlying both units is a 200-m-thick trachyte layer and, at the bottom, a lithic tuff 16-m thick (TPAO & UNOCAL 1990b; e.g., Ömer Şahintürk, pers. comm. 2005), (3) the Nemrut 8 drill hole (elevation: 2296.67 m) was drilled within the caldera. First, it cut a pumice layer 64-m thick. The underlying volcaniclastic sequence is as follows: a trachyte unit (36 m), a pumice layer (10 m), a thin scoria-basaltic tuff layer (64 m), another trachyte layer (106 m), a tuff layer (70 m), a vitric-tuff layer (14 m), a trachyte unit (95 m), and finally, a tuff layer (5 m) (TPAO & UNOCAL 1990c; e.g., Ömer Şahintürk, pers. comm. 2005).

Volume Estimates

Volume estimates were calculated using the equation V = thickness X deposition area. The volume estimates were made on the basis of the drilling data and field study. In respect to the tuff layer, we selected the minimum thickness from the three drill holes. The thickness of the Nemrut Ignimbrite (named tuff in the TPAO & UNOCAL project) is, on the basis of the project data, 70 m. We neglected the flattening ratio of fiammes in our calculation. The Nemrut Ignimbrite covers an area of 616 km^2. We estimate the volume of the Nemrut Ignimbrite to be about 43.1 km^3, which represents a minimum value without taking into account the 35% co-ignimbrite ash (Sparks & Walker 1977); if the 35% of lost dust is added, the original volume of the Nemrut ignimbrite can be roughly estimated at 58.2 km^3.

We can calculate the tephra deposits (pumice fallouts and pyroclastic surges) thus: total pumice thickness was 74 m (64 m + 10 m) during Phase 2 on the basis of the drill data. Plinian pumice-fall deposits cover an area of 60 km^2. We calculate a tephra amount of 4.5 km^3. Therefore, during Phase 2, the total volume of pyroclastic material is estimated as 62.6 km^3.

Interpretation and Discussion

We have analyzed and correlated columnar sections of pyroclastic material from the Nemrut stratovolcano. We note that the structural and textural parameters of the pyroclastics change frequently (Figures 5 & 13). Two ignimbrites, the initial and the main one, have been identified around the Nemrut stratovolcano. However, within the study area, only one ignimbrite unit related to caldera development has been identified. We cannot, at present, elucidate the origin of the initial ignimbrite because evidence for the initial ignimbrite is first identified 28 km SW of the caldera. In other words, we cannot observe any contact zone between the initial and main ignimbrites. Finally, the main ignimbrite has been identified, but the initial ignimbrite and its source could not have been connected to the caldera.

It is marked that fallout deposits are dominant on the eastern flank of the caldera (Figure 2). We suppose that after cone building reached its maximum level, high-energy Peléan-type eruptions occurred and the main ignimbrite became dominant. Following the pyroclastic flows, plinian pumice-fall deposits (P.F.D.1-P.F.D.2) formed. The extensive distribution of the pumice-fall deposits at the eastern side of caldera and the geometry of the eruption column are of particular importance since they indicate the prevalent wind direction at the same time of their formation. Regional variations in the thickness of the plinian fall deposits indicate that the fallout fan extends to the east.

In both of the ignimbrites, colour, thickness and clast-size variations are observed in proximal and distal areas. While the Nemrut Ignimbrite is yellow and brown in proximal areas, it is black, blackish-grey and dark brown in distal areas. Clasts belonging to the P.F.D.2 are up to ~35 cm on the eastern flank of the caldera, but their sizes are only ~5 cm 5.5 km SE of the caldera rim.

Within the ignimbrites, pumice fragments are recrystalized due to welding and are flattened by lithostatic pressure; consequently, they contain well-developed fiamme structures (Figure 9b). Fiammes developed after deposition. Their flattening ratios are dependent upon temperature, chemical composition, and degree of compaction. Locally, the fiammes were exposed to lateral pressures and became inclined; thus they can be used to ascertain the direction of the source (Cas & Wright 1988). On the basis of some measurements of fiamme inclination, the source is determined to have been the caldera. However, our data in this regard (indicating the caldera as source) may be accidental because we cannot measure fiamme flattening statistically. Colour

	Initial Ignimbrite	Main Ignimbrite							
		Phase 1 plinian pumice falls							
		Unite 1				Unite 2			
Features		P1	P2	P3	A1	P4	S	A2	P5
Thickness (m)	40	3	1	0.8	0.2	1	3	0.1	1.5
Min. distances by source (km)	28 (SW)	5.5 (S)	5.5 (S)	5.5 (S)	5.5 (S)	5.5 (S)	17 (S)	2.5 (NE)	2.5 (NE)
Welding degree	low-high	–	–	–	–	–	–	–	–
Max. pumis grain-size (cm)	15	4	7	7	–	–	1	–	4
Max. lithic grain-size (cm)	1–1.5	–	–	–	–	0.3	–	2	–
Fiammes (H/L)	2/20	–	–	–	–	–	–	–	–

	Palaeosol	Main Ignimbrite					Palaeosol	Main Ignimbrite	
		Phase 2						Phase 3	
			Nemrut Ignimbrite						
Features		P.F.D.1	Bottom	Middle	Top	P.F.D.2		P6	A3
Thickness (m)	0.3	2.5	7	5	1	2.5	0.05	1.5	–
Min. distances by source (km)	5.5 (SE)	8 (SE)	5.5 (NE) 6 (SE)	5.5 (S)	by source	5.5 (SE)	5.5 (S)	2 (E)	5 (S)
Welding degree	–	–	middle-high	high	low-middle	–	–	–	–
Max. pumis grain-size (cm)	–	8	3	30	9	–	–	3	–
Max. lithic grain-size (cm)	–	–	4	25	3	3	–	–	–
Fiammes (H/L)	–	–	–	0.4/6.5	–	–	–	–	–

Figure 13. Textural parameters of the Nemrut stratovolcano pyroclastics. Key to abbreviations: P– pumice layers; A– ash-fall deposits; S– scoria-fall deposits; SE– southeast; NE– northeast; S– south; E– east; P.F.D. – plinian pumice-fall deposits.

variations are widespread. Vertical colour variations within the two ignimbrites, from green to grey, black to grey, brown to yellow, are controlled by thermal conductivity differences during flow and immediately thereafter (Cas & Wright 1988).

Within the study area, only one ignimbrite unit related to the caldera formation has been identified. The Nemrut Ignimbrite is widespread, with an approximate areal extent of minimum 616 km^2. This unit overlies a variety of lava types that developed in the pre-caldera stage; for

example, many of the trachytic and rhyolitic domes (and environs) located around the caldera are overlain by ignimbrite. So, while the slopes of domes facing the caldera have lower-angle morphologies, those facing away from the caldera have quite steeply sloping morphologies. For example, the NI overlies the trachytic Kirkor Dome to the southwest of the caldera. The presence of ignimbrite in trough areas on this dome, the fact that its original position is preserved, the "plastering" of the pyroclastic material onto the walls of the dome, and the mineralogic-petrographic similarity to ignimbrite in the walls of the Nemrut stratovolcano, confirm that these rocks are from the same unit; that it escaped from the nearly vertical, ~ 450-m-high dome walls proves that flow energy was high.

There have been two major proposals concerning the development of the Nemrut caldera: collapse (Güner 1984; Yılmaz *et al.* 1998), and collapse and eruption at the same time (Maxon 1936; Özpeker 1973). Most calderas form as a result of voluminous pyroclastic eruptions. Initial plinian fall deposits are followed by pyroclastic flows.

Many types of eruptions occur in two well-defined stages in response to pressure variations within the magma chamber during eruption (Druitt & Sparks 1984). Also, Roche & Druitt (2001) provided a simple quantitative model and proposed that 10–30% of the chamber volume may be erupted before the chamber becomes underpressured and a caldera forms. Field observations suggest that there was an energy discharge from the magma chamber toward the surface at the Nemrut stratovolcano. The data (gathered from vertical columnar sections within the pyroclastic materials) concerning eruption energy is discernable through the stratovolcano's various eruption phases and processes, as presented above. Thus, after the formation of a major eruption column, pre-ignimbrite plinian pumice-fall deposits (P.F.D.1) occurred and a short period later, a pyroclastic flow. Ash clouds with dense gas, pumice, and ash concentrations accompanied the flow and completed their descent after the ignimbrite came to rest. After this huge magma discharge, the pressure of the magma chamber diminished to a level below lithostatic pressure, the upper side of cone collapsed, and formation of the caldera was completed.

Dikes that had played an active role in the formation of the caldera are observed at several locations on the southwest, west and north flanks of the caldera, but are masked by pyroclastics and lava flows on the eastern flank of the caldera. Highly explosive eruptions expanded in all directions from the main cone which, of course, existed prior to caldera formation. The ignimbrites cover some dome and lava vents, but were not preserved atop many volcanic structures as a function of flow direction. The ignimbrite passed over all nearby dome structures and with great energy, proceeded to cover an area exceeding 616 km^2. It is possible to see remnants of the ignimbrite flow that passed over the Kirkor Dome (Karaoğlu 2003) – the highest dome in the area – both near the peak of the dome and also on slopes situated opposite the flow direction (Figure 14).

The continuity of Nemrut lavas and the spread of the initial ignimbrite 80 km away from its source to Bitlis Valley affected the present configuration of the boundaries of the Lake Van basin and thus modified the regional morphology (Innocenti *et al.* 1976; Şaroğlu & Güner 1981; Yılmaz 1989). Although the ignimbrite is aerially extensive around the stratovolcano, unequivocal data concerning whether or not the primary ignimbrite unit induced caldera formation were not acquired in this study. However, it is clear that the Nemrut caldera formed after the main ignimbrite eruptions, since the Nemrut caldera – as calderas elsewhere – developed following a discharge of pumice and ignimbrite. It is suggested that ignimbrite was discharged from the upper part of the magma chamber, thus triggering caldera formation.

Summary and Conclusions

The evolution of the Nemrut volcano can be summarized as follows:

1. The physical evolution of the stratovolcano may be subdivided into three stages, namely pre-caldera, post-caldera and late stages.
2. The first lava belonging to the Nemrut volcanism is present in Bitlis Valley. The lavas that erupted subsequently were trachytic and basaltic flows. Since the upper parts of these flows are covered by NI, their relations to other flows could not be ascertained during this study.
3. Soil formation at two separate levels within the pyroclastic sequence indicates that the volcano was quiescent for at least two long periods.

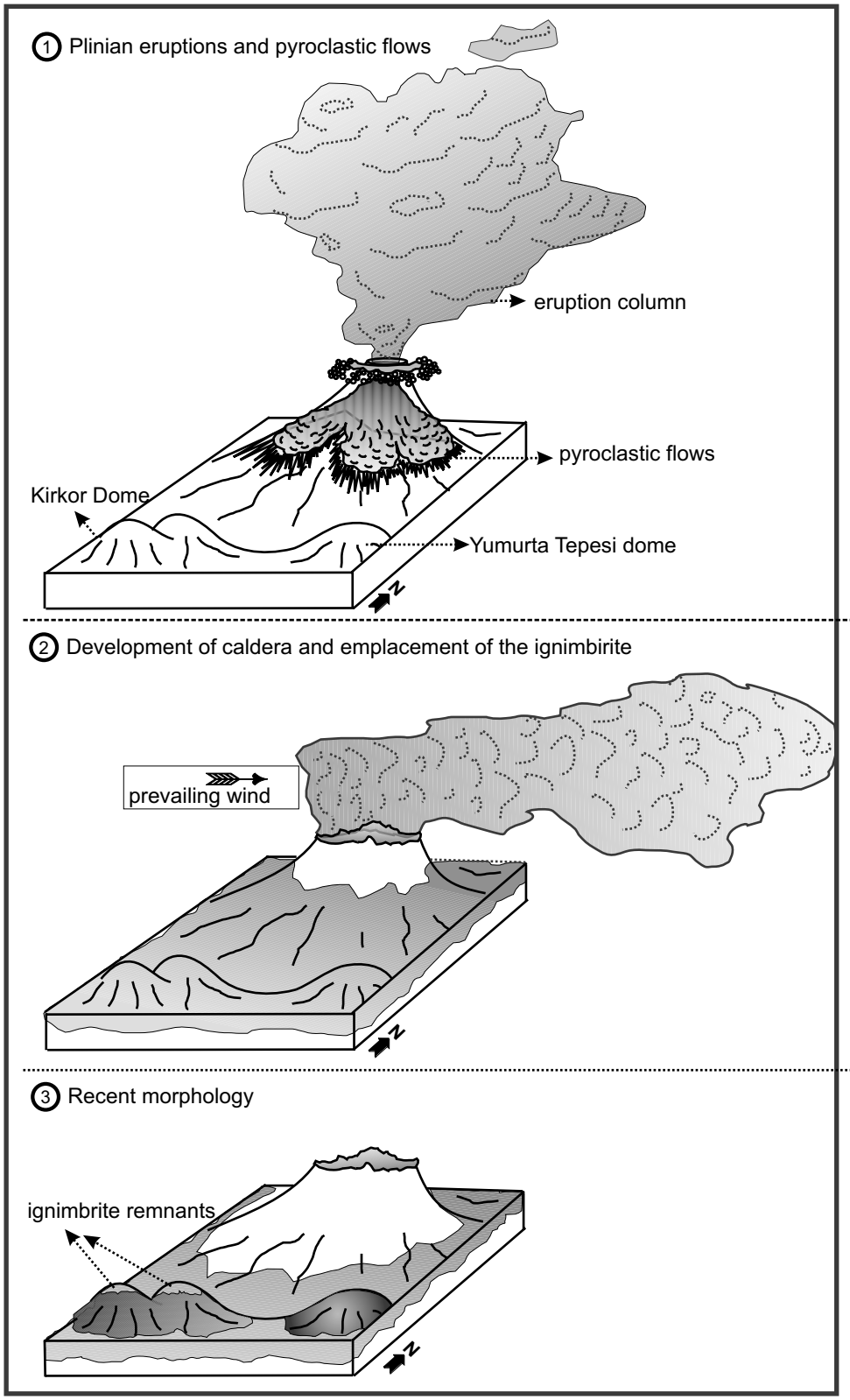

Figure 14. Development of the Nemrut caldera and plinian eruptions.

4. The NI has been observed in three distinct layers, simply designated bottom, middle, and top.
5. Fiamme structures and recrystallized pumice present in well-fused layers indicate that the ignimbrite flow was extremely hot at formation.
6. The volume of Nemrut Ignimbrite and tephra during phase 2 is estimated at 62.6 km^3.
7. Ash layers within the study area may have been products of the main Nemrut cone, but the possibility of derivation from outside the study area cannot be ruled out. In the İncekaya tuff ring, 17 km south of the Nemrut stratovolcano, ash, scoria and other pyroclastic products are of basaltic composition. It is possible that these basaltic pyroclastic materials were transported into the study area by aeolian processes following explosive eruptions.

Acknowledgements

We gratefully acknowledge support of our fieldwork by TÜBİTAK-YDABAG (Project No: 102Y103) and the Directorate of the Yüzüncü Yıl University Research Project Fund (Project No: Mim-051). The authors are indebted to Steve Mittwede, Cahit Helvacı, Çağlar Özkaymak, Yahya Çiftçi, Serkan Üner, Ömer Şahintürk, Vural Oyan, Fuat Erkül, and Mustafa Toker for reviewing the manuscript and making helpful suggestions to improve it. Special thanks to Rolf Schumacher, Nilgün Güleç and Erdin Bozkurt for their kind help regarding and important comments on an earlier version of the manuscript.

References

AYDAR, E., GOURGAUD, A., ULUSOY, I., DIGONNET, F., LABAZUY, P., ŞEN, E., BAYHAN, H., KURTTAŞ, T. & TOLLUOĞLU, A.Ü. 2003. Morphological analysis of active Mount Nemrut stratovolcano, eastern Turkey: evidences and possible impact areas of future eruption. *Journal of Volcanology and Geothermal Research* **123**, 301–312.

BOZKURT, E. 2001. Neotectonics of Turkey – a synthesis. *Geodinamica Acta* **14**, 3–30.

BOZKURT, E. 2003. Origin of NE-trending basins in western Turkey. *Geodinamica Acta* **16**, 61–81.

CAS, R.A.F. & WRIGHT, J.V. 1988. *Volcanic Successions*. Chapman and Hall Ltd., London.

DEWEY, J.F., HEMPTON, M.R., KIDD, W.S.F., ŞAROĞLU, F. & ŞENGÖR, A.M.C. 1986. Shortening of continental lithosphere: the neotectonics of Eastern Anatolia - a young collision zone. *In*: COWARD, M.P. & RIEA, A.C. (eds), *Collision Tectonics*. Geological Society, London, Special Publications **19**, 3–36.

DRUITT, T.H. & SPARKS, R.S.J. 1984. On the formation of calderas during ignimbrite eruptions. *Nature* **310**, 679–681.

ERCAN, T., FUJITANI, T., MOLSUDA, J., NOTSU, K., TOKEL, S. & TADAHIDE, U.İ. 1990. Doğu ve Güneydoğu Anadolu Neojen-Kuvaterner volkanitlerine ilişkin yeni jeokimyasal, radyometrik ve izotopik verilerin yorumu [Interpretation of new geochemical, radiometric and isotopic data from the Neogene–Quaternary volcanics in eastern and southeastern Turkey]. *MTA Dergisi* **110**, 143–164 [in Turkish with English abstract].

GUDMUNDSSON, A. 2002. Emplacement and arrest of sheets and dykes in central volcanoes. *Journal of Volcanology and Geothermal Research* **116**, 279–298.

GÜLEÇ, N., HILTON, D. R. & MUTLU, H. 2002. Helium isotope variations in Turkey: relationship to tectonics, volcanism and recent seismic activities. *Chemical Geology* **187**, 129–142.

GÜNER, Y. 1984. Nemrut yanardağının jeolojisi, jeomorfolojisi ve volkanizmanın evrimi [The geology, geomorphology and volcanic evolution of the Nemrut volcano]. *Jeomorfoloji Dergisi* **12**, 23–65 [in Turkish].

INNOCENTI, F., MAZZUOLI, R., PASQUARE, G. & REDICAT DE DROZOLO VILLARI, L. 1976. Evolution of the volcanism in the area of interaction between the Arabian, Anatolian and Iranian plates (Lake Van, Eastern Turkey). *Journal of Volcanology and Geothermal Research* **1**, 103–112.

KARAKHANIAN, A., DJRBASHIAN, R., TRIFONOV, V., PHILIE, H., ARAKELION, S. & AVAGIAN, A. 2002. Holocene-historical volcanism and active faults as natural risk factors for Armenia and adjacent countries. *Journal of Volcanology and Geothermal Research* **113**, 319–344.

KARAOĞLU, Ö. 2003. *Nemrut Kalderası Kuzeyi'nin Jeolojisi, Mineralojisi ve Petrografisi [The Geology, Mineralogy and Petrography of the Northern Nemrut Caldera]*. MSc Thesis, Yüzüncü Yıl University, Van, Turkey [in Turkish with English abstract, unpublished].

KARAOĞLU, Ö., ÖZDEMİR,Y. & TOLLUOĞLU, A.Ü. 2004. Physical evolution, emplacement of ignimbrite and characteristic eruption types of Nemrut Stratovolcano: a caldera system at Eastern Anatolia-Turkey. *Proceedings of the 5th International Symposium on Eastern Mediterranean Geology*, 1287–1290.

KESKİN, M., PEARCE, J.A. & MITCHELL, J.G. 1998. Volcano-stratigraphy and geochemistry of collision-related volcanism on the Erzurum-Kars Plateau, northeastern Turkey. *Journal of Volcanology and Geothermal Research* **85**, 355– 404.

KOÇYİĞİT, A., YILMAZ, A., ADAMIA, S. & KULOSHVILI, S. 2001. Neotectonics of East Anatolian plateau (Turkey) and lesser Caucasus: implication for transition from thrusting to strike-slip faulting. *Geodinamica Acta* **14**, 177–195.

MAXON, J.H. 1936. *Nemrut Gölü [The Nemrut Lake].* General Directorate of Mineral Research and Exploration (MTA) Publications **5**, 49–57 [in Turkish with English abstract].

NOTSU, K., FUJITONI, T., UI, T., MATSUDA, J. & ERCAN, T. 1995. Geochemical features of collision-related volcanic rocks in central and eastern Anatolia, Turkey. *Journal of Volcanology and Geothermal Research* **64**, 171–192.

OSWALT, F. 1912. *Armenian. Handbuch der regionalen Geologie,* volume 10. Heidelberg.

ÖZDEMİR, Y. 2003. *Nemrut Kalderası Güneyi'nin Jeolojisi, Mineralojisi ve Petrografisi [The Geology, Mineralogy and Petrography of the Southern Nemrut Caldera].* MSc Thesis, Yüzüncü Yıl University, Van, Turkey [in Turkish with English abstract, unpublished].

ÖZDEMİR, Y., KARAOĞLU, Ö., TOLLUOĞLU A.Ü. & GÜLEÇ, N. 2005. Volcanostratigraphy and petrogenesis of the Nemrut stratovolcano (East Anatolian High Plateau): the most recent post-collisional volcanism in Turkey. *Chemical Geology* [in press].

ÖZPEKER, İ. 1973. Nemrut Yanardağının petrojenezi [Petrogenesis of the Nemrut volcano]. *TÜBİTAK 4. Bilim Kongresi, Yer Bilimleri Seksiyonu Bildiriler Kitabı*, 1–17 [in Turkish].

PEARCE, J.A., BENDER, J.F., DE LONG, S.E., KIDD, W.S.F., LOW, P.J., GÜNER, Y., ŞAROĞLU, F., YILMAZ, Y., MOORBATH, S. & MITCHELL, J.G. 1990. Genesis of collision volcanism in eastern Anatolia, Turkey. *Journal of Volcanology and Geothermal Research* **44**, 189–229

ROCHE, O. & DRUITT, T.H. 2003. Onset of caldera collapse during ignimbrite eruptions. *Earth and Planetary Science Letters* **191**, 191–202.

ŞAROĞLU, F. & GÜNER, Y. 1981. Doğu Anadolu'nun jeomorfolojik gelişimine etki eden öğeler; jeomorfoloji, tektonik, volkanizma ilişkisi [Factors affecting the geomorphological evolution of eastern Turkey: relationships between geomorphology, tectonics and volcanism]. *Geological Bulleting of Turkey* **24**, 39–50 [in Turkish with English abstract].

ŞEN, P.A, TEMEL, A. & GOURGAUD, A. 2004. Petrogenetic modeling of Quaternary post- collisional volcanism: a case study of central and eastern Anatolia. *Geological Magazine* **141**, 81–98.

ŞENGÖR, A.M.C. & KIDD, W.S.F. 1979. Post-collisional tectonics of the Turkish-Iranian plateau and a comparison with Tibet. *Tectonophysics* **55**, 361–376.

ŞENGÖR, A.M.C. & YILMAZ, Y. 1981. Tethyan evolution of Turkey: a plate tectonic approach. *Tectonophysics* **75**, 181–241.

SEREFHAN, 1597. *Serefname: Kurt Tarihi* (translated from Arabic to Turkish by M. Emin Bozarslan), 4th Edition (1990). Hasat Yayınları, İstanbul.

SPARKS, R.S.J. 1976. Grain size variations in ignimbrites and implications for the transport of pyroclastic flows. *Sedimentology* **23**, 147–188.

SPARKS, R.S.J. & WALKER, G.P.L. 1977. The significance of vitric-enriched air-fall ashes with crystal-enriched ignimbrites. *Journal of Volcanology and Geothermal Research* **2**, 329–341.

TPAO & UNOCAL 1990a. Nemrut-5 Jeotermal Kuyusu Kuyu Tamamlama Raporu [Drilling Report of Nemrut-5 Drill-hole]. *Türkiye Petrolleri A.O. Jeotermal Müdürlüğü* [in Turkish, unpublished].

TPAO & UNOCAL 1990b. Nemrut-7 Jeotermal Kuyusu Kuyu Tamamlama Raporu [Drilling Report of Nemrut-7 Drill-hole]. *Türkiye Petrolleri A.O. Jeotermal Müdürlüğü* [in Turkish, unpublished].

TPAO & UNOCAL 1990c. Nemrut-8 Jeotermal Kuyusu Kuyu Tamamlama Raporu [Drilling Report of Nemrut-8 Drill-hole]. *Türkiye Petrolleri A.O. Jeotermal Müdürlüğü* [in Turkish, unpublished].

YILMAZ, Y. 1989. Comparison of young volcanic associations of western and eastern Anatolia formed under a compressional regime: a review. *Journal of Volcanology and Geothermal Research* **44**, 69–87.

YILMAZ, Y., GÜNER, Y. & ŞAROĞLU, F. 1998. Geology of the Quaternary volcanic centres of the East Anatolia. *Journal of Volcanology and Geothermal Research* **85**,173–210.

YILMAZ, Y., ŞAROĞLU, F. & GÜNER, Y. 1987. Initiation of the neomagmatism in East Anatolia. *Tectonophysics* **137**, 177–199.

Received 04 February 2005; revised typescript accepted 09 August 2005